ELECTRONIC SUPPLEMENTARY INFORMATION

Tensile and Torsional Elastomer Fiber Artificial Muscle by Entropic Elasticity with Thermo-Piezoresistive Sensing of Strain and Rotation by Single Electric Signal

Run Wang,‡[a] Yanan Shen,‡[b] Dong Qian[c], Jinkun Sun,[b] Xiang Zhou,[c] Weichao Wang[a] and Zunfeng Liu*[ab]

[a]State Key Laboratory of Medicinal Chemical Biology, College of Chemistry and College of Electronic Information and Optics Engineering, Key Laboratory of Functional Polymer Materials, Nankai University, Tianjin 300071, China
[b]College of Pharmacy, Nankai University, Tianjin, 300071, China
[c]Department of Mechanical Engineering, The University of Texas at Dallas, Richardson, TX 75080, USA
[d]Department of Science, China Pharmaceutical University, Nanjing, Jiangsu, 211198, China
‡ These authors contributed equally to this work.
*Corresponding author E-mail: liuzunfeng@nankai.edu.cn

This file includes:

S1. Theoretical section for the torsional actuation

First we consider the torque balance before the application of the heat. As mentioned in the section 2.2, the CNT$_m$/elastomer fiber was first connected to a thin elastomer fiber and then twist was inserted. The total twist can be given as $\theta = \tau\left(\frac{1}{k_1} + \frac{1}{k_2}\right)$, in which τ is the applied torque before heating, and k_1, k_2 are the torsional stiffness for the CNT$_m$/elastomer fiber and thin elastomer fiber, respectively. After the heat is applied, k_1 increases to $k_1^{'}$. This increase can be explained by the formula for torsional stiffness, given as $\frac{GJ}{l}$, with l the length, G the shear modulus and J the polar second moment of area of the cross-section, $J = \frac{\pi d^4}{32}$. When heat is applied, l will reduce due to increase in elastic modulus, d will correspondingly increase due to incompressibility and G will increase due to entropic elasticity. Therefore, overall k_1 increases.

Since the fibers are torsionally tethered at both ends after twist insertion and thermal activation, the total twist remains unchanged. The torque τ in the fibers need to be changed to $\tau^{'}$ in order to satisfy this constraint, *i.e.*,

$$\tau\left(\frac{1}{k_1} + \frac{1}{k_2}\right) = \tau^{'}\left(\frac{1}{k_1^{'}} + \frac{1}{k_2}\right) \quad (1).$$

From eqn. (1), the updated torque due to heating is given as

$$\tau^{'} = \tau \frac{\left(1+\frac{k_2}{k_1}\right)}{\left(1+\frac{k_2}{k_1^{'}}\right)} \quad (2),$$

and the ratio of the twist angles $\left(\frac{\theta_1^{'}}{\theta_1}\right)$ in the CNT$_m$/elastomer fiber after and before heating can be given as

$$\frac{\theta_1^{'}}{\theta_1} = \frac{\frac{\tau^{'}}{k_1^{'}}}{\frac{\tau}{k_1}} = \frac{\frac{\tau}{k_1^{'}}\frac{\left(1+\frac{k_2}{k_1}\right)}{\left(1+\frac{k_2}{k_1^{'}}\right)}}{\frac{\tau}{k_1}} = \frac{k_1}{k_1^{'}}\frac{\left(1+\frac{k_2}{k_1}\right)}{\left(1+\frac{k_2}{k_1^{'}}\right)} = \frac{k_1+k_2}{k_1^{'}+k_2} \quad (3).$$

Eqn. (3) shows that the change in the twist angle in the CNT_m/elastomer fiber is inversely proportional to the change in the torsional stiffness in the same fiber. An increase from k_1 to $k_1^{'}$ leads to a reduction in the twist angle in the CNT_m/elastomer fiber, which explains the observed untwist. The torsional actuation in this work is based on a twisted, non-coiled fiber muscle, which is different from the stretch-induced twist increase for a coiled configuration, where stretch-twist coupling could be involved with decrease in length, leading to twist increase in a coiled configuration.[1]

The twist angle change ($\Delta\theta_1$) of the CNT_m/elastomer fiber can be derived from Eqn. (3) above, given as

$$\Delta\theta_1 = \frac{k_1' - k_1}{k_1' + k_2} \frac{k_2}{k_1 + k_2} \theta \qquad (4).$$

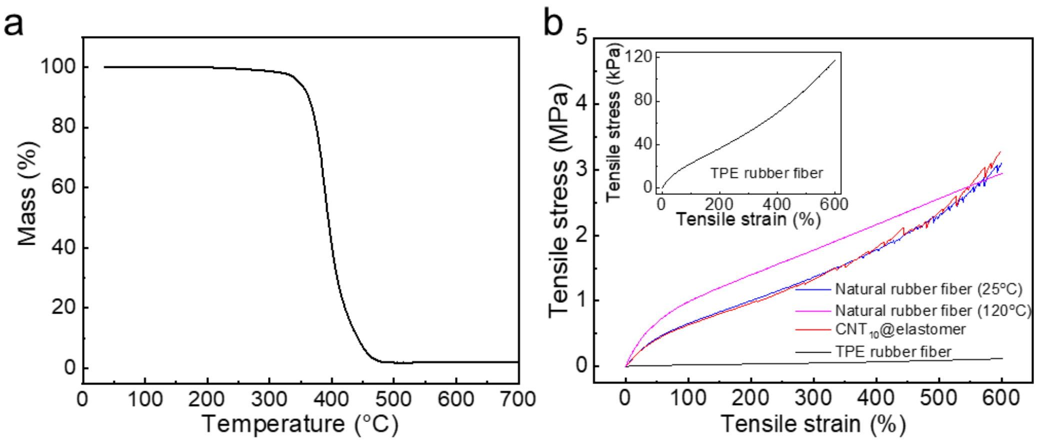

Fig. S1.

(a) Percent mass loss as a function of temperature for the natural rubber fiber in thermal gravimetric analysis measurement at a heating rate of 20°C/min in N_2 atmosphere. (b) The stress-strain curves for the natural rubber fiber at 25°C and 120°C, TPE rubber at 25°C, and the CNT_{10}/elastomer fiber at 25°C. The inset of (b) shows a stress-strain curve of the TPE rubber at a smaller scale of y axis.

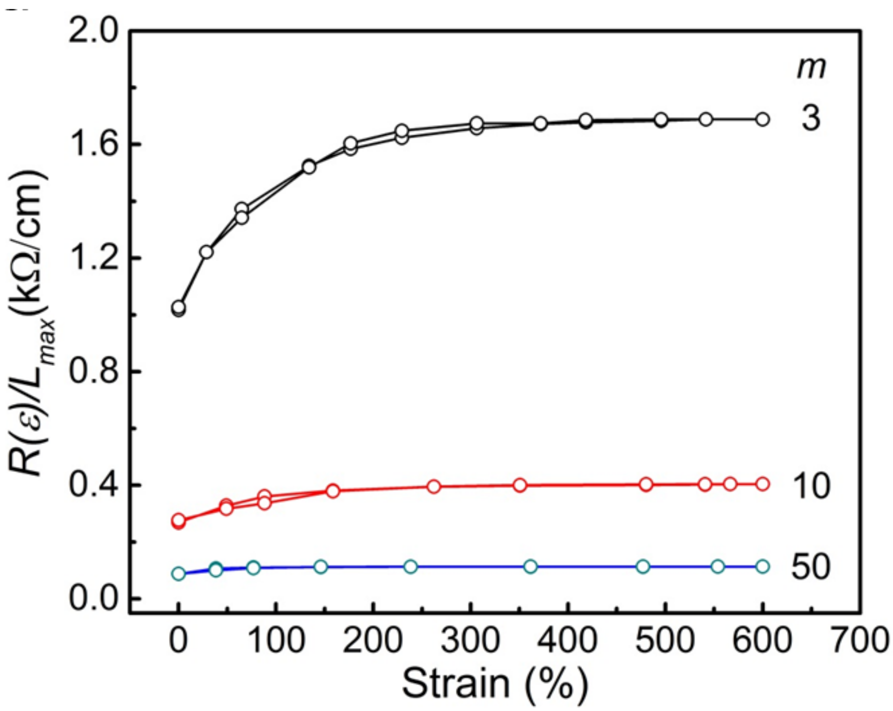

Fig. S2.

(a) Length-normalized resistance as a function of strain for the CNT_m/elastomer fiber.

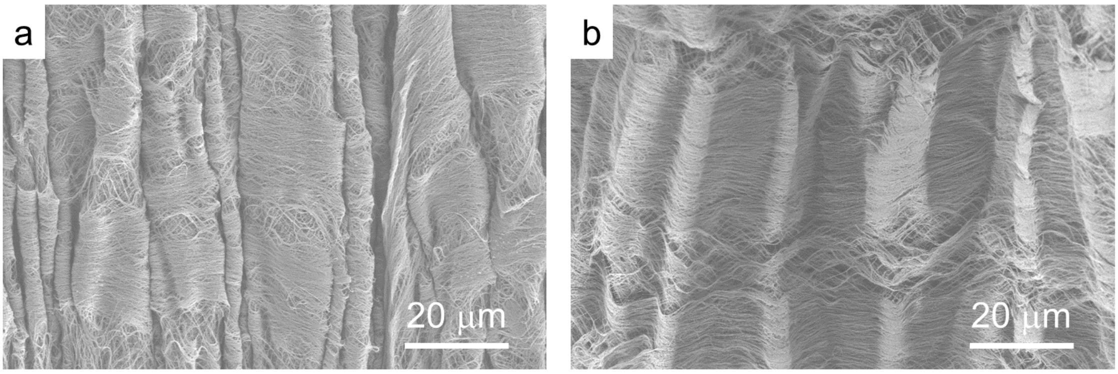

Fig. S3.
SEM images of the CNT_{10}/elastomer at (a) 0% and (b) 200% strains, showing that the contacting content of buckles decreased with increase in strain.

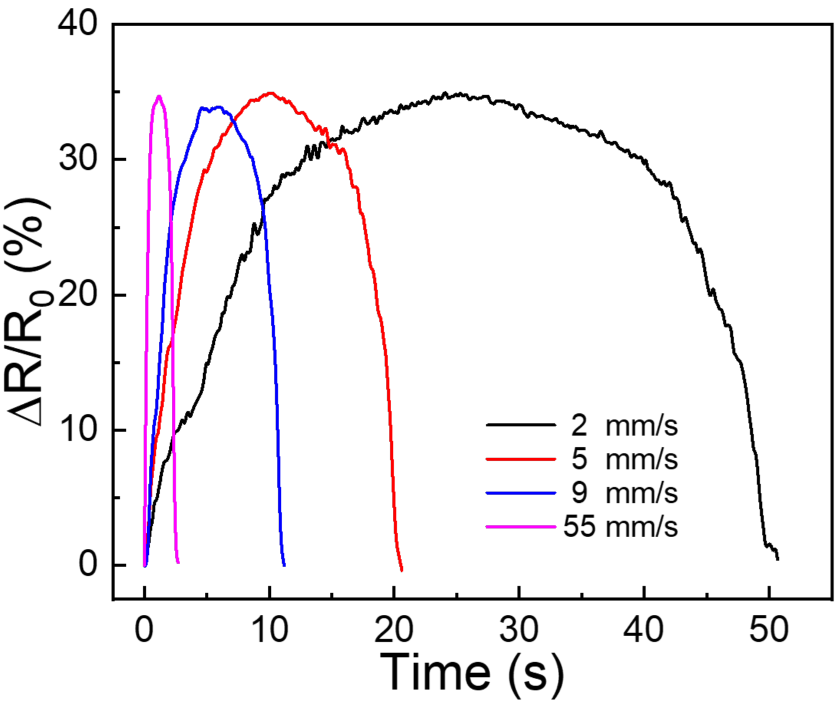

Fig. S4.
Percent resistance change of the CNT_{10}/elastomer fiber as a function of time during stretching up to 110% strain at different stretch rates. The initial length of CNT_{10}/elastomer fiber was 4.5 cm.

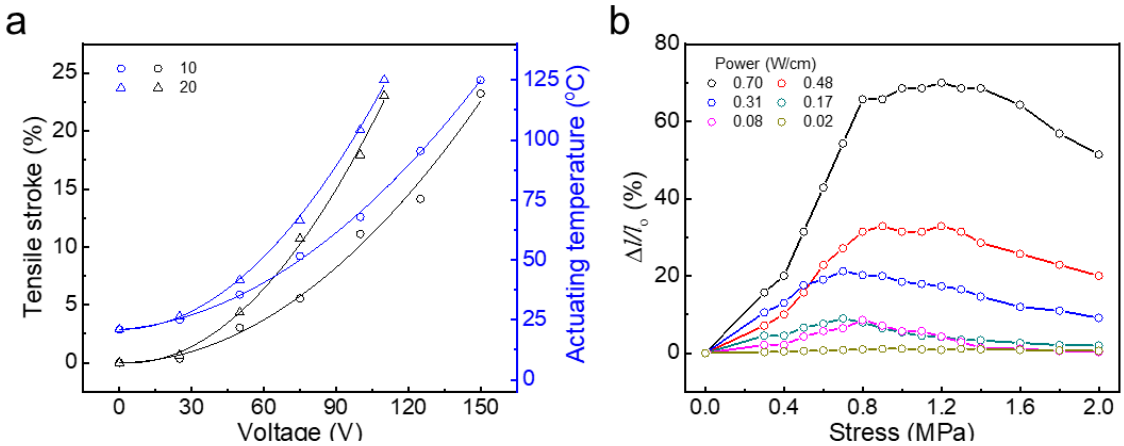

Fig. S5.

(a) Tensile stroke and temperature as a function of applied voltage for CNT_m/elastomer muscles at isobaric stress of 0.8 MPa for m=10 and 20. (b) Apparent tensile stroke ($\Delta l/l_o$) of a CNT_{10}/elastomer muscle as a function of isobaric stress under different input electric power.

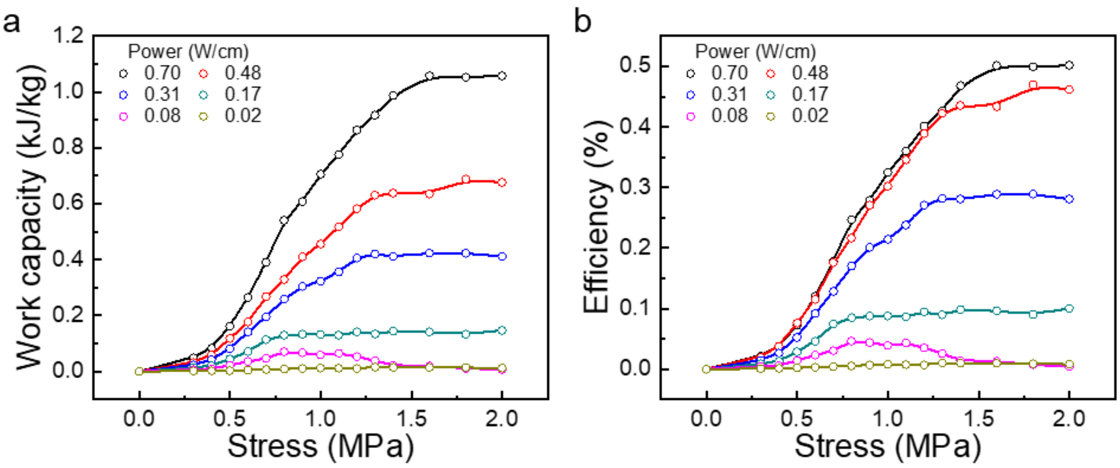

Fig. S6.

Work capacity (a) and efficiency (b) of a CNT_{10}/elastomer muscle as a function of isobaric stress under different input electric power.

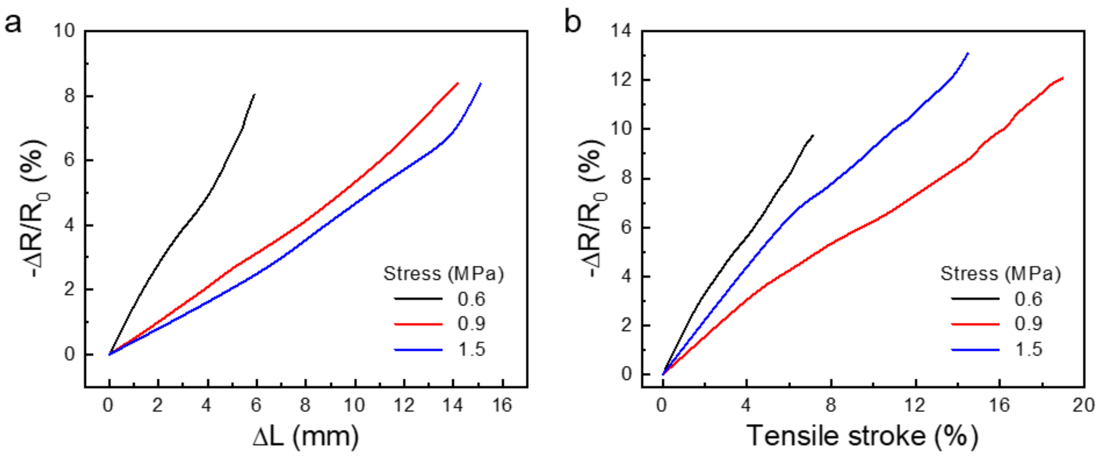

Fig. S7.

(a, b) Percent resistance decrease as a function of muscle length change (a) and as a function of tensile stroke (b) during electro-thermal actuation of a CNT_{10}/elastomer muscle at different isobaric stresses. The applied voltage is 45 V, and the CNT_{10}/elastomer muscle is not twisted.

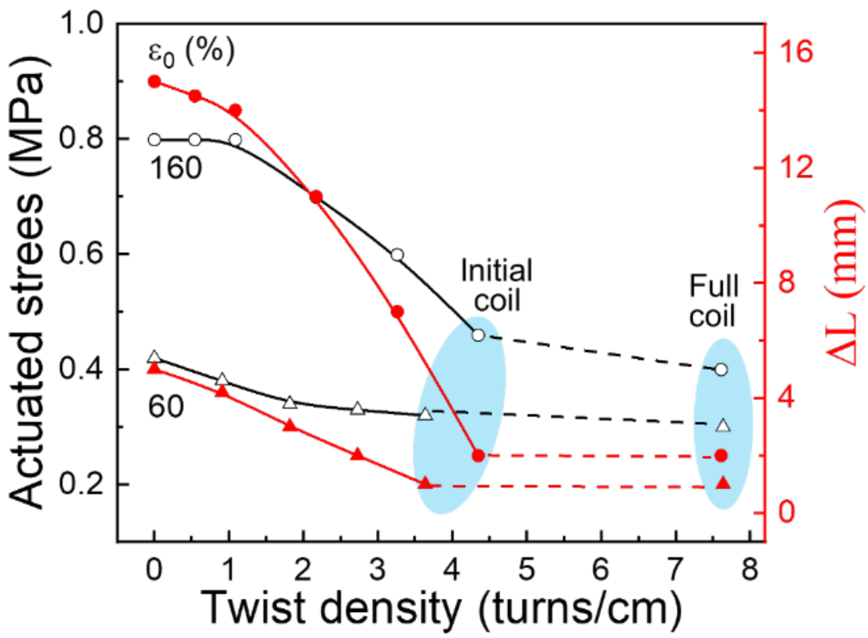

Fig. S8. The stress used to keep the same value of the initial length before actuation, and length decrease during actuation as a function of inserted twist for the torsional CNT_{10}/elastomer muscle. The applied electric power was 0.62 W/cm, the initial muscle elongation was ε_0 = 160% and 60%, respectively, for different inserted twist. The initial muscle length before actuation is the same for different inserted twist.

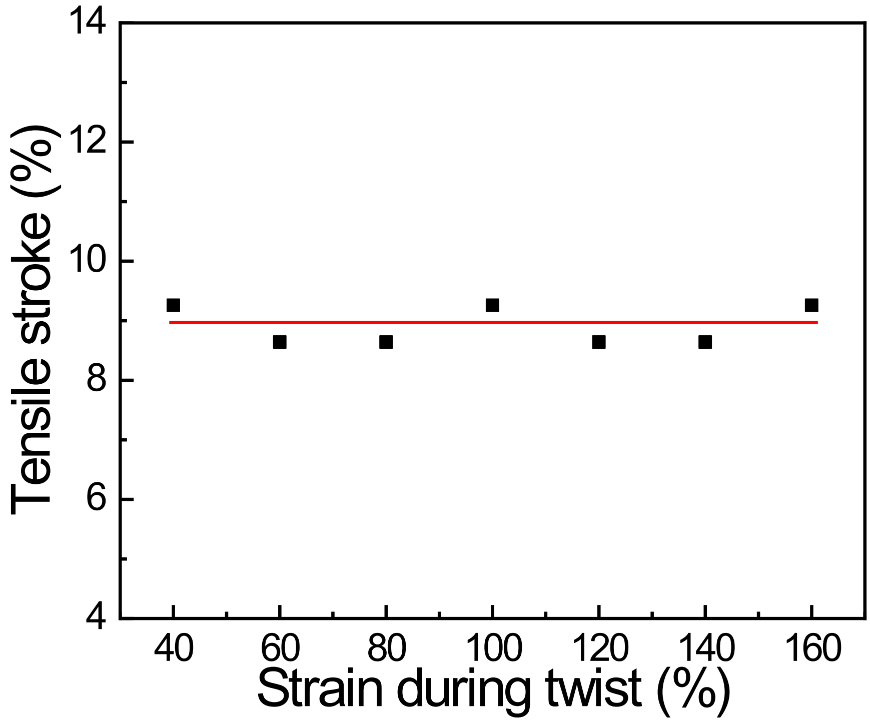

Fig. S9.

The tensile stroke of a twisted CNT_{10}/elastomer muscle that was twisted at different isometric strain. The muscle was isobarically loaded with 0.5 MPa weight and electro-thermally actuated under 0.31 W/cm electric power.

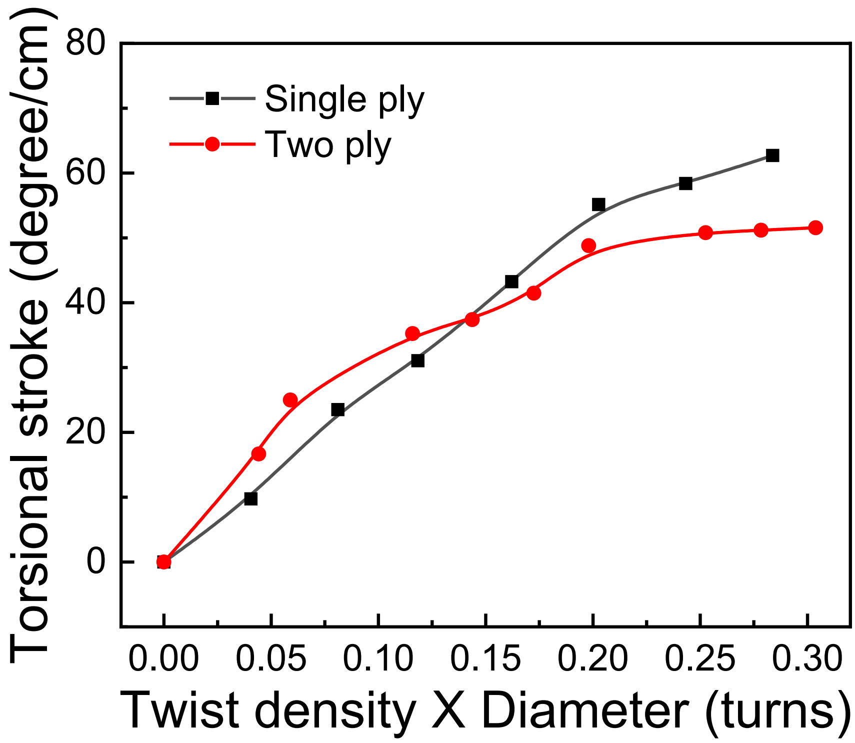

Fig. S10.

Torsional stroke as a function of the product of twist density and the fiber diameter.

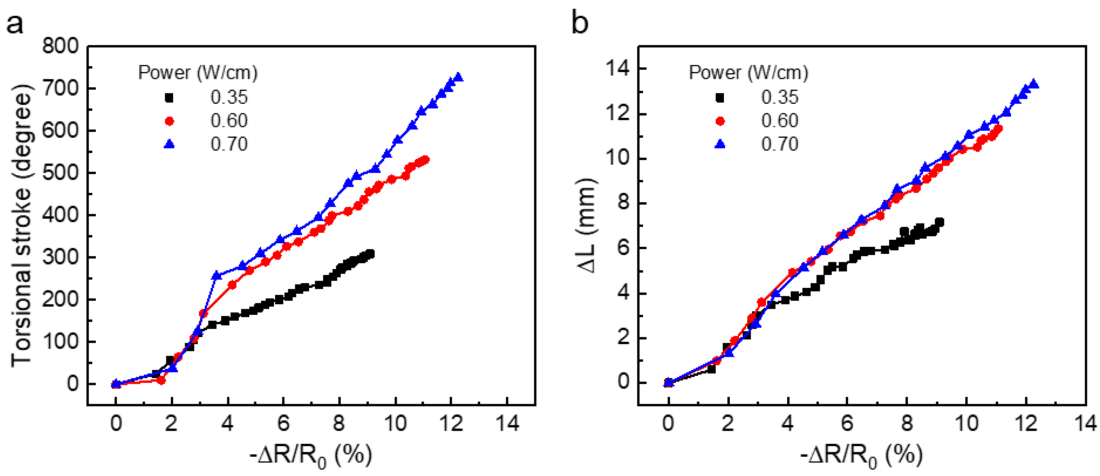

Fig. S11.

(a, b) Torsional stroke (a) and muscle length change (b) as function of percent resistance change during electro-thermal actuation of a torsional CNT_{10}/elastomer muscle at different applied electric power. The twist density of the CNT_{10}/elastomer was 1.7 turns/cm, and the isobaric load was 0.8 MPa.

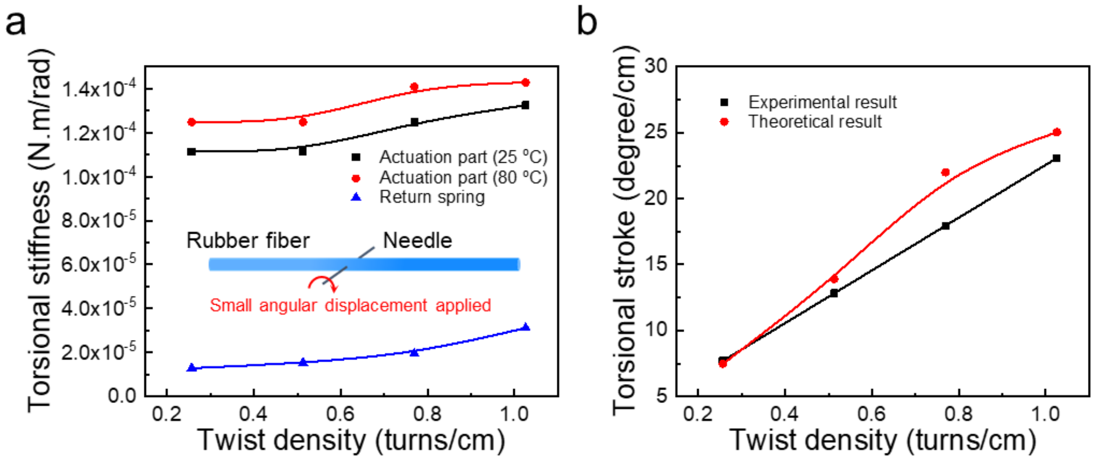

Fig. S12.

(a) Torsional stiffness as a function of twist density for a CNT_{10}/elastomer muscle. The inset in (a) schematically illustrates the apparatus for measuring the torsional stiffness of the actuation part and the return spring of a torsional CNT_m/elastomer muscle. (b) Comparison of experimentally measured and theoretically calculated torsional strokes for a CNT_{10}/elastomer muscle under isobaric load of 0.3 MPa. The non-loaded muscle fiber is 3.0 cm in length and 2.0 mm in diameter, and the return spring fiber is 3.8 cm in length and 0.8 mm in diameter.

Table S1 Comparison of performance of the artificial muscle in this work with other elastomer based artificial muscles.

Materials	Stimulus	Optimal actuation		Tensile stroke (%)	Torsional stroke (°/cm)	Sensing function	Maximum work capacity	Efficiency (%)	Ref.
		Stress (MPa)	Strain (%)						
VHB 4910	Electro-filed (412 MV/m)	-	(300, 300)	61 thickness 158 area	No	No	-	-	2
	Electro-filed (239 MV/m)	-	(500, 75)	68 thickness 215 area	No	No	-	-	
VHB 4910	Electro-filed (18 kV, 1620 MV/m)	-	(200, 200)	167 area	No	No			3
IPN VHB 4910	Electro-filed (65 MV/m)	2.6 kg	(0, 0)	10	No	No	0.013 kJ/kg		4
Wacker Elastosil	Electro-filed (29.5 MV/m)	0.1 kg	(0, 0)	5.2	No	No	-	-	5
Wacker Elastosil	Electro-filed (2.5 kV, 90 MV/m)	10.0 kg	(20, 20)	3.4	No	No	1620 kJ/m^3	-	6
SEBS	Electro-filed (10.3 MV/m)	0.01	-	4.1	21.8	No	-	-	7
LCE	Thermal (35-200°C)	0	0	55	No	No	0.003 kJ/kg 3.6 kJ/m^3	-	8
LCE	Thermal (100-140°C)	0.14	20	37	No	No	-	-	9
	Thermal (50-130°C)	0.048	10	28	No	No	-	-	
IPN-LCE	Thermal (40-140°C)	22.0	40	50	No	No	1.83 kJ/kg 1268 kJ/m^3		10
LCE	Thermal (25-150°C)	0.84	35	63	No	No	731 kJ/m^3	-	11
LCE	Thermal (85-125°C)	0.3	82	37	No	No	-		12
LCP	Photo-thermal	2.3 g	800	64	No	No	81 kJ/m^3		13
LCE/CNT	Electro-thermal (150°C)	0.84	-	12	No	No	97 kJ/m^3		14
LCE	Thermal (25-150°C)	0.29	140	28	No	No	0.05 kJ/kg 97 kJ/m^3		15
Spandex rubber	Electro-thermal (RT-70°C)	9.6	100	12.4	No	No	0.64 kJ/kg	3.2	16
Polyacrylic ester	Electro-thermal (RT-80°C)	3.7	-	21	No	No	1.16 kJ/kg	-	17
Spandex rubber	Thermal (20-130°C)	1.96 N	-	14	No	No	0.598 kJ/kg	-	18
Nature rubber	Electro-thermal	1.0	-	5	No	No	-	0.02	19

Nature skeletal muscle	Chemical energy	0.1-0.35	-	20-40	-	Motor neuron system	0.04 kJ/kg 40 kJ/m^3	40	20
Nature rubber	Electro-thermal (25-125°C)	0.8	180	23	87.5	Thermo-Piezoresistive strain sensor	1.06 kJ/kg 1026 kJ/m^3	0.5	This work

IPN: interpenetrating polymer networks; SEBS: styrene-ethylene-butylene-styrene; LCE: liquid crystal elastomer; LCP: liquid crystal polymer; CNT: carbon nanotube sheet; ATP: adenosine triphosphate. Torsional stroke is normalized by muscle length.

Table S2 Comparison of the artificial muscle in this work with other actuating systems.

Actuator	Structure	Stimulus	Sensor	One single signal (stimulus and sensor)	Feedback loop control	Ref.
Bending	Microchannel and corrugation	Pneumatic	Resistance strain sensor	Separately	No	21
Bending	Bimorph	Magnetic filed	Piezoresistance sensor	Separately	No	22
Tensile	Coil	Electro-thermal	Capacitive strain sensor	Separately	No	23
Bending	Bimorph	Moisture, thermal, and light	Resistance sensor	Separately	No	24
Bending	Sandwich	Electric filed	Resistance sensor	Separately	No	25
Tensile	Tendril	Heat	Piezoresistive strain sensor	Separately	No	26
Bending	Bimorph	Electro-thermal	Pyroelectric temperature and piezoresistive strain sensor	Separately	No	27
Expansion	Sandwich	Dielectric	Capacitive sensor	Together	No	28
Bending	Bimorph	Electro-thermal	Resistance strain sensor	Together	No	29
Bending	solid on one side and slit on the other	Pneumatic	Optoelectronic strain sensor	Separately	Yes	30
Expansion	Sandwich	Dielectric	Capacitive sensor	Together	Yes	31
Tensile	Cylindrical	Chemical energy	Muscle spindle	Together	Yes	32
Tensile and torsional	Twisted fiber	Electro-thermal	Thermo-piezoresistive strain sensor	Together	Yes	This work

References

1. A. Ghatak and L. Mahadevan, *Phys. Rev. Lett.*, 2005, **95**, 057801.
2. R. Pelrine, R. Kornbluh, Q. Pei and J. Joseph, *Science*, 2000, **287**, 836-839.
3. C. Keplinger, J.-Y. Sun, C. C. Foo, P. Rothemund, G. M. Whitesides and Z. Suo, *Science*, 2013, **341**, 984-987.
4. G. Kovacs, L. Düring, S. Michel and G. Terrasi, *Sensor Actuat. A-Phys*, 2009, **155**, 299-307.
5. H. S. Jung, S. Y. Yang, K. H. Cho, M. G. Song, C. T. Nguyen, H. Phung, U. Kim, H. Moon, J. C. Koo and J.-D. Nam, *Int. J. Control Autom*, 2017, **15**, 25-35.
6. S. Hau, G. Rizzello and S. Seelecke, *Extreme Mech. Lett.*, 2018, **23**, 24-28.
7. Z. Liu, S. Fang, F. Moura, J. Ding, N. Jiang, J. Di, M. Zhang, X. Lepró, D. Galvão and C. Haines, *Science*, 2015, **349**, 400-404.
8. T. H. Ware, M. E. McConney, J. J. Wie, V. P. Tondiglia and T. J. White, *Science*, 2015, **347**, 982-984.
9. D. L. Thomsen, P. Keller, J. Naciri, R. Pink, H. Jeon, D. Shenoy and B. R. Ratna, *Macromolecules*, 2001, **34**, 5868-5875.
10. H.-F. Lu, M. Wang, X.-M. Chen, B.-P. Lin and H. Yang, *J. Am. Chem. Soc.*, 2019, **141**, 14364-14369.
11. H. Kim, J. M. Boothby, S. Ramachandran, C. D. Lee and T. H. Ware, *Macromolecules*, 2017, **50**, 4267-4275.
12. Z. Pei, Y. Yang, Q. Chen, E. M. Terentjev, Y. Wei and Y. Ji, *Nat. Mater.*, 2014, **13**, 36-41.
13. X. Pang, L. Qin, B. Xu, Q. Liu and Y. Yu, *Adv. Funct. Mater.*, 2020, **30**, 2002451.
14. H. Kim, J. A. Lee, C. P. Ambulo, H. B. Lee, S. H. Kim, V. V. Naik, C. S. Haines, A. E. Aliev, R. Ovalle‐Robles and R. H. Baughman, *Adv. Funct. Mater.*, 2019, **29**, 1905063.
15. T. Ware and T. White, *Polym. Chem.*, 2015, **6**, 4835-4844.
16. J. Foroughi, G. M. Spinks, S. Aziz, A. Mirabedini, A. Jeiranikhameneh, G. G. Wallace, M. E. Kozlov and R. H. Baughman, *ACS Nano*, 2016, **10**, 9129-9135.
17. J. Mu, C. Hou, G. Wang, X. Wang, Q. Zhang, Y. Li, H. Wang and M. Zhu, *Adv. Mater.*, 2016, **28**, 9491-9497.
18. S. Y. Yang, K. H. Cho, Y. Kim, M.-G. Song, H. S. Jung, J. W. Yoo, H. Moon, J. C. Koo and H. R. Choi, *Smart Mater. Struct.*, 2017, **26**, 105025.
19. P.-J. Cottinet, D. Guyomar, J. Galineau and G. Sebald, *Sensor Actuat. A-Phys*, 2012, **180**, 105-112.
20. J. D. Madden, N. A. Vandesteeg, P. A. Anquetil, P. G. Madden, A. Takshi, R. Z. Pytel, S. R. Lafontaine, P. A. Wieringa and I. W. Hunter, *IEEE J. Ocean. Eng.*, 2004, **29**, 706-728.
21. J. C. Yeo, H. K. Yap, W. Xi, Z. Wang, C. H. Yeow and C. T. Lim, *Adv. Mater. Technol.*, 2016, **1**, 1600018.
22. H.-P. Phan, T. Dinh, T.-K. Nguyen, A. Vatani, A. R. Md Foisal, A. Qamar, A. R. Kermany, D. V. Dao and N.-T. Nguyen, *Appl. Phys. Lett.*, 2017, **110**, 144101.
23. H. Wang, Z. Liu, J. Ding, X. Lepró, S. Fang, N. Jiang, N. Yuan, R. Wang, Q. Yin and W. Lv, *Adv. Mater.*, 2016, **28**, 4998-5007.
24. H. Cheng, F. Zhao, J. Xue, G. Shi, L. Jiang and L. Qu, *ACS Nano*, 2016, **10**, 9529-9535.
25. K. Kruusamäe, P. Brunetto, S. Graziani, A. Punning, G. Di Pasquale and A. Aabloo, *Polym. Int.*, 2010, **59**, 300-304.
26. M. Kanik, S. Orguc, G. Varnavides, J. Kim, T. Benavides, D. Gonzalez, T. Akintilo, C. C. Tasan, A. P. Chandrakasan and Y. Fink, *Science*, 2019, **365**, 145-150.
27. X. Q. Wang, K. H. Chan, Y. Cheng, T. Ding, T. Li, S. Achavananthadith, S. Ahmet, J. S. Ho and G. W. Ho, *Adv. Mater.*, 2020, **32**, 2000351.
28. T. A. Gisby, B. M. O'Brien and I. A. Anderson, *Appl. Phys. Lett.*, 2013, **102**, 193703.
29. M. Amjadi and M. Sitti, *Adv. Sci.*, 2018, **5**, 1800239.

30. H. Zhao, K. O'Brien, S. Li and R. F. Shepherd, *Sci. Robot.*, 2016, **1**, eaai7529.
31. S. Rosset, B. M. O'Brien, T. Gisby, D. Xu, H. R. Shea and I. A. Anderson, *Smart Mater. Struct.*, 2013, **22**, 104018.
32. M. Hulliger, in *Reviews of Physiology, Biochemistry and Pharmacology, Volume 101*, Springer, 1984, pp. 1-110.